ACS Infectious Diseases

Article

pubs.acs.org/journal/aidcbc

Inhibiting the β-Lactamase of *Mycobacterium tuberculosis* (Mtb) with Novel Boronic Acid Transition-State Inhibitors (BATSIs)

Sebastian G. Kurz,[†] Saugata Hazra,[‡] Christopher R. Bethel,[§] Chiara Romagnoli,[∥] Emilia Caselli,[∥] Fabio Prati,*[,∥] John S. Blanchard,*[,⊥] and Robert A. Bonomo*[,#,∇,§]

[†]Department of Medicine, Tufts Medical Center, 600 Washington Street, No. 257, Boston, Massachusetts 02111, United States

[‡]Department of Biotechnology, Indian Institute of Technology Roorkee (IITR), Roorkee, Uttarakhand 247667, India

[§]Research Service, Louis Stokes Cleveland Veterans Affairs Medical Center, 10701 East Boulevard, Cleveland, Ohio 44106, United States

[∥]Department of Life Science, University of Modena and Reggio Emilia, Via Campi 183, 41100 Modena, Italy

[⊥]Department of Biochemistry, Albert Einstein College of Medicine, 1300 Morris Park Avenue, Bronx, New York 10461, United States

[#]Department of Molecular Biology and Microbiology and [∇]Department of Biochemistry and Department Pharmacology, Case Western Reserve University School of Medicine, Cleveland, Ohio 44106, United States

Ⓢ *Supporting Information*

ABSTRACT: BlaC, the single chromosomally encoded β-lactamase of *Mycobacterium tuberculosis*, has been identified as a promising target for novel therapies that rely upon β-lactamase inhibition. Boronic acid transition-state inhibitors (BATSIs) are a class of β-lactamase inhibitors which permit rational inhibitor design by combinations of various R1 and R2 side chains. To explore the structural determinants of effective inhibition, we screened a panel of 25 BATSIs to explore key structure−function relationships. We identified a cefoperazone analogue, EC19, which displayed slow, time-dependent inhibition against BlaC with a potency similar to that of clavulanate (K_i* of 0.65 ± 0.05 μM). To further characterize the molecular basis of inhibition, we solved the crystallographic structure of the EC19-BlaC(N172A) complex and expanded our analysis to variant enzymes. The results of this structure−function analysis encourage the design of a novel class of β-lactamase inhibitors, BATSIs, to be used against *Mycobacterium tuberculosis*.

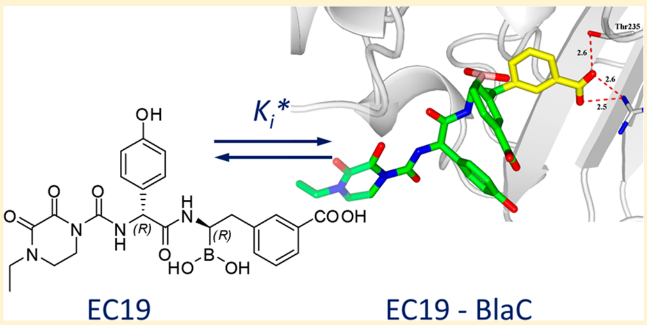

KEYWORDS: *Mycobacterium tuberculosis, β-lactamase inhibition, boronic acid transitional-state inhibitors, acylation high-energy intermediate, deacylation high-energy intermediate, cefoperazone analogue EC19*

Currently, four-drug regimens are the cornerstone of treatment against infections with *Mycobacterium tuberculosis* (Mtb), achieving cure rates that approach 95%.[1−3] Unfortunately, therapeutic challenges arise as a result of drug resistance. Because of the long treatment duration and the ability of *Mycobacteria* spp. to readily adapt to changes in their microenvironment, the emergence of resistance is inevitable. Against multidrug-resistant (MDR) and extensively drug-resistant (XDR) strains of Mtb, chemotherapeutic choices are limited and new options are being sought.[4] The concurrence of infection by human immunodeficiency virus, HIV, and Mtb creates a serious global challenge. Recent progress in antiretroviral therapy is hampered by the increasing frequency of drug-resistant strains of Mtb.

Presently, β-lactams and their combination with β-lactam inhibitors are being explored for the treatment of Mtb. The chromosomal β-lactamase, BlaC, is responsible for resistance to β-lactam antibiotics of multiple classes.[5,6] BlaC, which is capable of inactivating a broad range of penicillins and cephalosporins, belongs to Ambler class A, the members of which are usually susceptible to inhibitors such as clavulanic acid.[6] Indeed, the combination of meropenem and clavulanate was found to be effective in sterilizing Mtb cultures, including XDR strains.[7] Furthermore, BlaC appears to be intolerant of substitutions that alter substrate profiles and confer resistance to clavulanic acid inactivation.[8] Notwithstanding, a detailed understanding of structural determinants of effective inhibition may lead to the development of more potent inhibitors. Upon the basis of these considerations, we anticipate that novel β-lactamase inhibitors that possess favorable pharmacodynamic and pharmacokinetic properties will be effective against BlaC and will play an important role in treating drug-resistant Mtb infections in the near future.[9]

Received: January 11, 2015
Published: March 19, 2015

Boronic acid transition-state inhibitors (BATSIs) are a class of β-lactamase inhibitors that have been studied and optimized for a variety of β-lactamase enzymes.[10−15] By binding covalently to the active-site nucleophile of the enzyme, the boronate adduct sterically and electronically resembles the tetrahedral high-energy intermediate of the β-lactam hydrolysis reaction. Such inhibitors have been shown to complex the active site and lead to inhibition in a reversible, competitive manner (Scheme 1). BATSIs can also be synthesized so that they possess a side group which resembles R1 side chains of known β-lactams necessary for specific interaction with the enzyme. The variation of this side chain and the optional addition of an R2 group allow a rational inhibitor design.[16]

Scheme 1. Mechanism of Boronic Acid Transition-State Inhibitors[a]

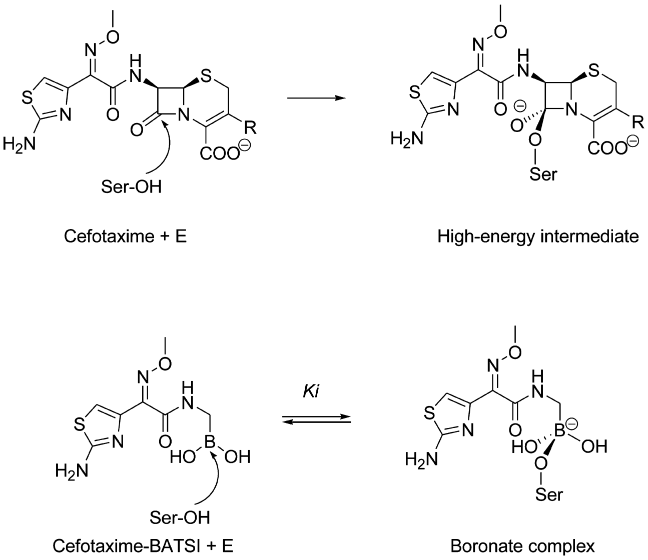

[a]The top row shows the formation of the tetrahedral high-energy intermediate of the cefotaxime−hydrolysis reaction. The bottom row shows the boronate complex formation of a cefotaxime-BATSI which resembles the tetrahedral high-energy intermediate.

To further elucidate the structural basis of effective inhibition, we used BATSIs to probe the active site of BlaC of Mtb. To this end, we tested a select panel of 25 BATSI compounds that carry different combinations of R1 and R2 side groups (Scheme 2), seven of which were newly synthesized. We determined key structural elements necessary for effective inhibition. We next expanded our analysis to variant enzymes with alterations in the carboxylate-binding regions. Our findings reveal that select BATSIs are effective biochemical inhibitors of BlaC; however, they rely on productive interactions with the carboxylate binding region of the enzyme. These results allow for the potential design of a novel class of β-lactamase inhibitors to be used in the treatment of Mtb and expand our repertoire of possible compounds to be used in therapy.

■ RESULTS AND DISCUSSION

The design strategy employed here started with the two reference compounds shown in Figure 1. The acetyl group of **1** was systematically replaced with R1 substituents present on the β-lactam ring of active penicillin and cephalosporin-like antibacterials (compounds **3**−**21**). In addition, a small number of ureido and sulfonamido derivatives were prepared (compounds **22**−**25**). These starting compounds were then further derivatized with one or two homologous *meta*-benzoic acid substituents (R2) to mimic the carboxylate group present on the larger heterocyclic fused ring of all β-lactam antibiotics. Finally, in the cefoperazone series, various phenolic, catecholic, and aniline rings were introduced as substituents of the phenolic group of the R1 side chain.

The enzyme inhibition by BATSIs is posited to follow slow reversible kinetics. On the basis of structural data, the model is represented according to eq 1

$$E + I \leftrightarrow E{:}I \leftrightarrow E{-}I^{\ddagger} \leftrightarrow E{-}I^{\ddagger\ddagger} \quad (1)$$

where E stands for β-lactamase enzyme, I stands for the inhibitor, E:I stands for the Michaelis complex, E−I‡ stands for the enzyme−inhibitor complex resembling the acylation high-energy intermediate, and E−I‡‡ stands for the deacylation high-energy intermediate, respectively. This model takes into account the crystallographic intermediates captured in SHV-1,[12] CTX-M-9, and CTX-M-14, respectively.[13] Using highly chromogenic nitrocefin as a substrate, we screened these 25

Scheme 2. General Scheme for the Synthesis of BATSI Compounds[a]

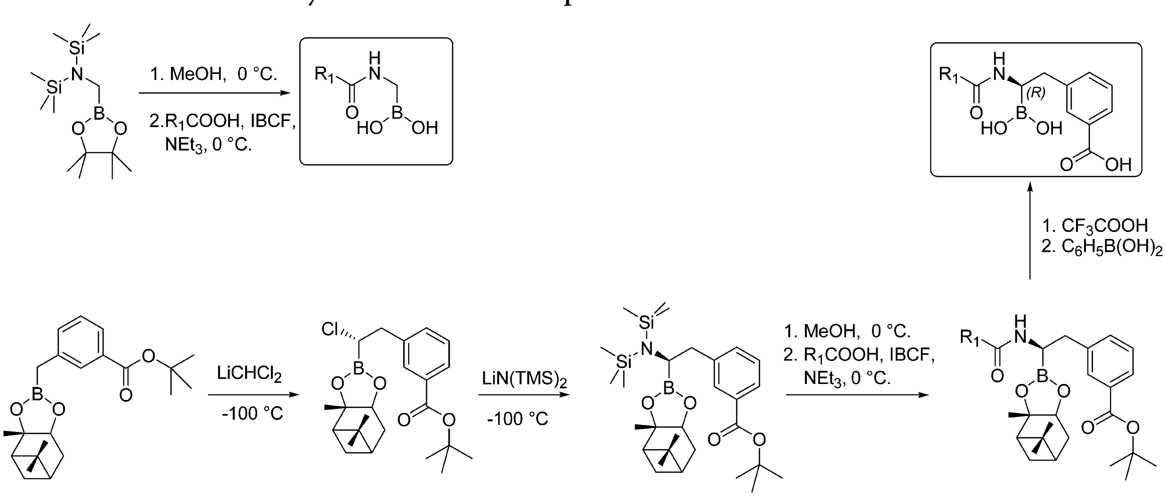

[a]See references in Table 1 and Supporting Information for details.

DOI: 10.1021/acsinfecdis.5b00003
ACS Infect. Dis. 2015, 1, 234−242

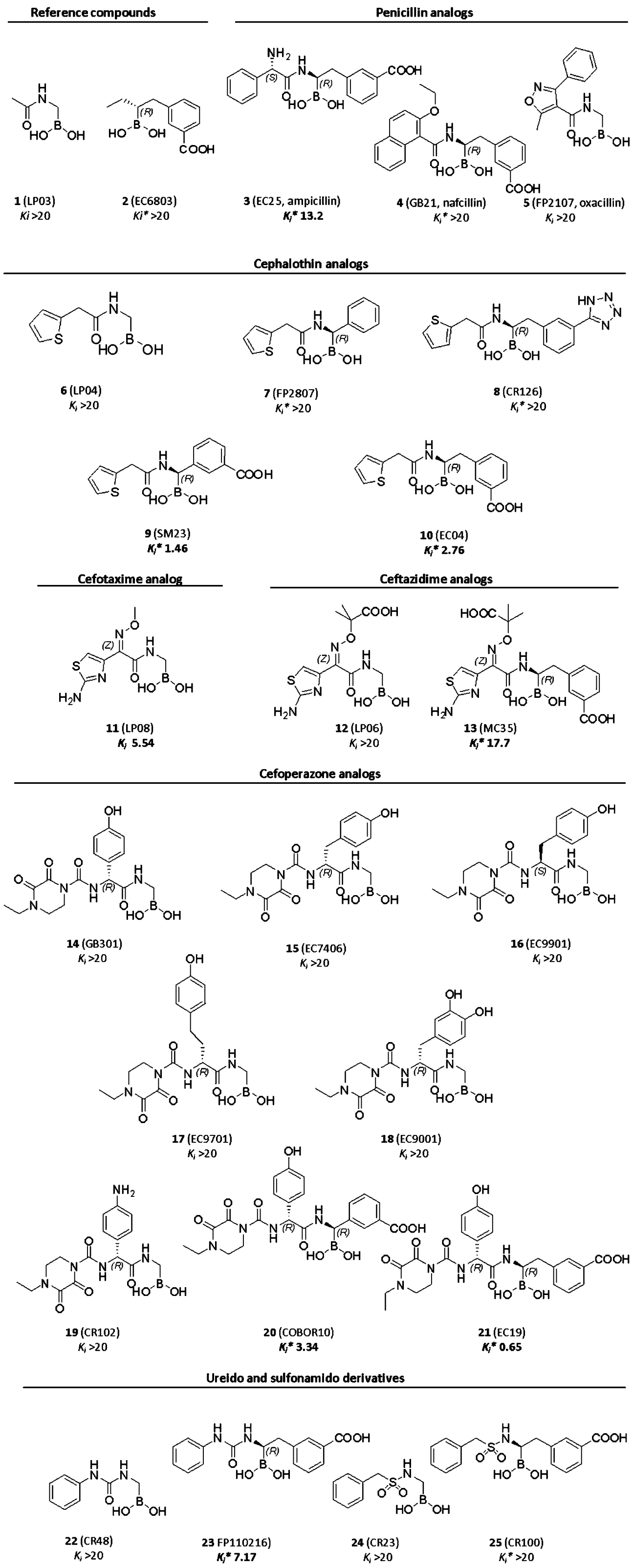

Figure 1. Structures and inhibition constants of the compounds tested as inhibitors of BlaC.

compounds both under initial velocity conditions and after 5 min of preincubation with BlaC. Inhibitor concentrations that reduce the substrate reaction by 50% were determined and expressed as K_i values for immediate inhibitory activity and K_i* values following 5 min of preincubation.

Both reference compounds **1** and **2** were devoid of inhibitory activity, even after 5 min. We identified eight with inhibitory activity, of which five inhibited BlaC at concentrations of less than 5 μM. Almost all of these active inhibitors contained a *meta*-benzoic acid R2 substituent. The only exception was the cefotaxime analog, compound **11**. In our experiments, compound **11** was the only rapid onset inhibitor whose K_i value was 5.5 ± 0.3 μM and decreased to K_i* = 4.1 ± 0.3 μM only after a 5 min incubation with BlaC. All other seven active compounds revealed negligible activity when testing the inhibition immediately following BlaC addition but revealed inhibition after a 5 min preincubation with enzyme. The only penicillin analog with activity after 5 min was the ampicillin analog, compound **3**, which possessed the benzoic acid R2 substituent. Of the cephalothin analogs, both compounds **9** and **10** showed activity after 5 min. Both compounds also have a benzoic acid R2 substituent, either directly attached to the boron-bearing carbon atom or with a methylene spacer for additional flexibility. The ceftazidime analog, compound **13**, was a relatively weak inhibitor.

Of the eight cefoperazone analogs, only compounds **20** and **21** showed inhibitory activity after a 5 min incubation with BlaC. This series explored different phenolic, catecholic, and aniline substituents to evaluate whether changing the stereochemistry (compound **16**) and side-chain length (compounds **15** and **17**) influenced the inhibitory activity. Compounds **20** and **21**, like those in the cephalothin series, differed only in the spacing of the benzoic acid R2 substituent with respect to the boron atom. In this case, however, the added methylene group reduced the K_i* value 5-fold, whereas in the cephalothin series, the opposite behavior was observed. Compound **21**, which we term EC19, exhibited the lowest K_i* value of all of the BATSIs, with a measured K_i* value of 0.65 ± 0.05 μM.

Finally, a small number of ureido- and sulfonamido-containing boronic derivatives were prepared and evaluated. Only ureido compound **23** exhibited inhibitory activity. Neither sulfonamide compound (**24** and **25**) exhibited activity, including compound **25** which contains the benzoic acid R2 substituent. These compounds are known to adopt a different orientation of the R2 substituent when bound to the AmpC β-lactamase.[17]

From these studies, we can make several general comments. First, there is a clear and strong improvement in inhibition when there is a benzoic acid as the R2 substituent; we postulate that this group interacts with BlaC where the conserved carboxyl group present in all β-lactams binds. It is also clear that the presence of this substituent in the inhibitors induces time-dependent inhibitor kinetics that is not observed with the single inhibitory compound lacking this feature (compound **11**). Second, the nature of the R1 substituent influences but is not the main driver of inhibitory activity. Different R1 groups were present in five different inhibitor series.

Interestingly, our results are quite different from other reports of BATSI inhibition of other class A and C β-lactamases. In the case of the *Acinetobacter*-derived ADC-7 cephalosporinase,[15] the achiral cephalothin showed favorable inhibitory activity that was enhanced by the addition of a phenyl group in the R2 position. Similar observations have been reported for the TEM-1 β-lactamase.[10] In the case of TEM-1, an aromatic R2 substituent allows for a favorable $\pi-\pi$ stacking interaction with the Tyr105 phenolic ring.[10] A tyrosine residue is found in the equivalent position in many class A β-lactamases.[18,19] The KPC-2 carbapenemase has a tryptophan at

DOI: 10.1021/acsinfecdis.5b00003
ACS Infect. Dis. 2015, 1, 234−242

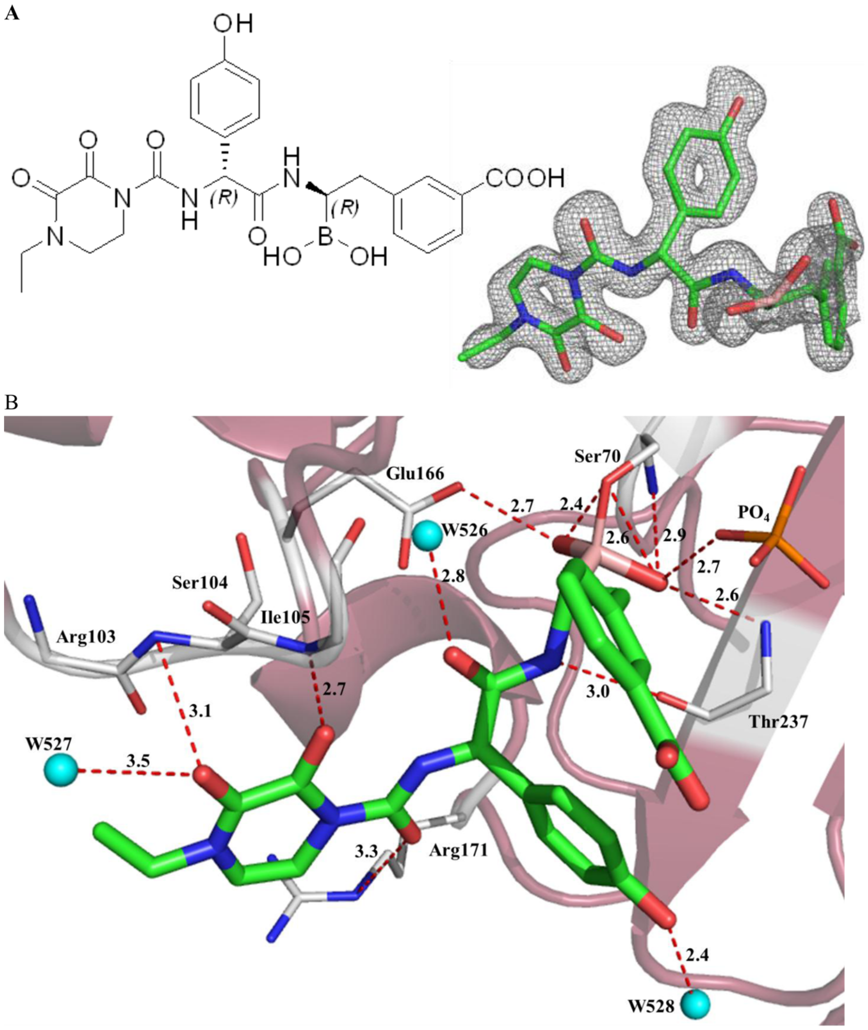

Figure 2. Crystal structure of BlaC with EC19 bound at the active site. Inhibitor atoms are colored by atom type. (A) Structure of EC19 (left) and EC19 modeled into the $F_o - F_c$ omit map contoured at 2.0σ. (B) Electrostatic interactions between covalently bound EC19 and BlaC.

the equivalent position that similarly stacks with aromatic substituents.[20] The structures of a large number of BlaC-substrate and -inhibitor complexes reveal that aromatic amino acid side chains are not present in the active site at an equivalent position. This position is occupied by an isoleucine residue instead, which may explain the lack of activity of compound **7**. Rather, we believe that the effectiveness of the benzoic acid-substituted BATSIs as BlaC inhibitors reflects their affinity for the carboxylate binding region of the active site. This may differentiate BlaC from other class A enzymes. In the crystal structure of BATSI covalently bound with the SHV-1 β-lactamase,[12] the R1 substituent is found in an orientation in which it interacts with the carboxylate binding region.

To this end, we tested the inhibitory effectiveness of compound **21** (EC19) as an inhibitor of variant forms of BlaC that possessed changes in the carboxylate binding pocket. In all previously characterized class A β-lactamases, this region is repesented by a K234-T235-G236 sequence motif (i.e., a KTG motif) and a nearby arginine residue, R244.[21] In BlaC, R244 is replaced with an alanine (A244). It was first shown for the TEM-1 β-lactamase that this positive charge could be replaced by arginine residues located proximally to R244.[22] In the case of BlaC, the function of R244 is served by R220, which provides the necessary positive charge and electrostatically interacts with the negatively charged carboxylate of the β-lactam substrates.[8] To investigate whether the R2 *meta*-benzoic acid substituent interacts with the carboxylate binding region of BlaC, we tested the inhibition of nitrocefin hydrolysis by R220A, R220S, and doubly substituted β-lactamase R220A, A244R (Table 2). These variants were constructed to investigate the impact of the positive charge (R220A, R220S) by relocalizing the positive charge from position 220 to 244. As a control, we also measured inhibition with the S130G variant enzyme which exhibits similar kinetic properties to the other variants but maintains the native carboxylate binding motif. Interestingly, we found that compound **21** is ineffective at inhibiting the R220A and R220S variants of BlaC yet retains potent inhibition against both the doubly substituted β-lactamase where the positive charge has been repositioned from residue 220 to residue 244 and the S130G BlaC retaining the native carboxylate binding site. These data argue that *meta*-benzoic acid R2 substituent binds as a mimic of the substrate carboxylate. Furthermore, these observations may point toward a potential mechanism to develop resistance against BATSI compounds.

Essentially, almost all of the active BATSIs exhibit time-dependent inactivation, a behavior that has been previously observed for other β-lactamases when inhibited with BATSIs

DOI: 10.1021/acsinfecdis.5b00003
ACS Infect. Dis. 2015, 1, 234−242

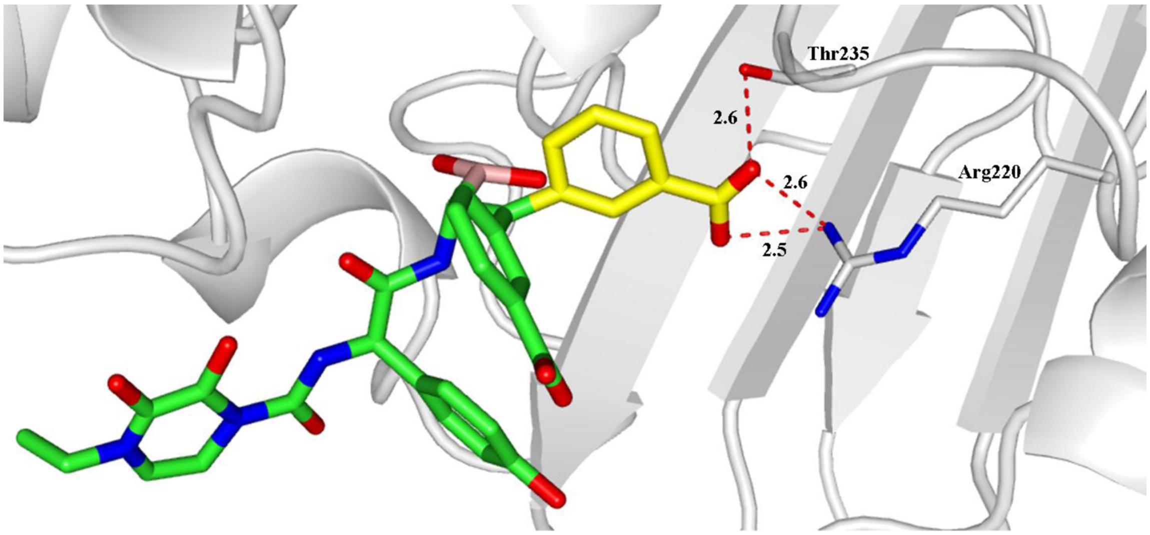

Figure 3. Proposed mode of binding EC19 with BlaC in solution. Only a modest rotation of the methylene group connecting the boron atom and the *meta*-benzoic acid substituent results in two hydrogen bonds formed with the side chains of Arg220 and Thr235.

that carry a stereogenic center.[23,24] To investigate this more thoroughly, we performed experiments in which the hydrolysis of nitrocefin by BlaC was determined as a function of inhibitor concentration, focusing on EC19 (compound **21**). As seen in Figure S1A, the initial rates are approximately similar at various EC19 concentrations, but after 150−200 s, the rates begin to decrease and at higher concentrations the reaction rates approach zero. These data were fit to a model where the inhibitors bind to the free BlaC and form an initial Michaelis complex, which then isomerizes in a slow step to generate a second complex. Using eq 4, we could calculate from these data values for k_{on} of 0.001 μM^{-1} s^{-1} and k_{off} of 0.0013 s^{-1}. (Our chemical interpretation of this kinetic model will be discussed below.) To test whether this time dependency also applied to the dissociation of the inhibitor from the complex and to ensure that the covalent complex was reversibly formed, we formed the complex ($10K_i$*) and tested for inhibitor release and the regaining of activity by diluting the complex 100-fold before adding nitrocefin to initiate the reaction. Using EC19, the reaction rate increased slowly, consistent with a reversible but very slow dissociation rate (Figure S2A). In contrast, when this experiment was performed with LP08 (compound **11**), the rate of hydrolysis of nitrocefin was essentially equal to the control reaction, where inhibitor was not added (Figure S2A). These kinetic results support our proposal that the time dependence of BATSIs containing the *meta*-benzoic acid R2 substituent is due to this binding and subsequent isomerization both in the association and dissociation reactions.

Finally, the influence of the R1 substituent on inhibitory potency is not mirrored in the efficiency of the corresponding *β*-lactam as the substrate for BlaC. Penicillins are in general better substrates for BlaC than cephalosporins.[6,25] For example, ampicillin exhibits a K_m value of 8 μM,[6,25] yet compound **3** exhibits one of the highest K_i* values of all active compounds tested. Cephalothin exhibits a K_m value of 150 μM; however, compound **10** exhibits a K_i* value of 2.7 ± 0.2 μM. Finally, cefotaxime exhibits a K_m value of 5.5 mM, yet compound **11** exhibits a K_i* value of 5.5 ± 0.3 μM. Similar observations have been reported for class A extended-spectrum *β*-lactamase CTX-M: the most potent BATSI inhibitor contained the R1 substituent of ceftazidime, one of the enzyme's least-favorable substrates.[13] To determine if this observation holds true for BlaC and cefoperazone, we evaluated cefoperazone as a substrate for BlaC. We did not detect any hydrolysis when testing concentrations of up to 100 μM. Furthermore, we tested to determine if this compound was a "slow substrate" for BlaC and thus an inhibitor of nitrocefin hydrolysis. Cefoperazone at a concentration of 10 μM did not inhibit nitrocefin hydrolysis. We hypothesize that the rigid structure of cefoperazone, with the dihydrothiazine ring fused to the *β*-lactam ring, may prevent the optimal interaction of both the carboxylate and the R1 substituent. In the case of the BATSI inhibitors described here, the *meta*-benzoic acid R2 substituent and R1 diketopiperazine are connected by bonds that allow for free rotation of the two groups, thus allowing for optimal alignment and interaction within the BlaC active site. In this setting, the more complex R1 substituents of the cephalosporins may allow for more specific interactions with BlaC that complement the interaction of the *β*-lactam carboxylate with the carboxylate binding site. In a broader view, BATSI inhibitors are not mimicking the natural substrate of the enzyme but rather the high-energy intermediate product of the enzymatic reaction.

Crystal Structure. Co-crystallization of wild-type BlaC with EC19 was prevented by the dissolution of the crystal in DMSO-containing inhibitor solution. However, the compound was successfully trapped in the N172A variant protein which additionally resulted in larger crystals, and the structure was resolved at 1.4 Å. There was clear electron density between the Ser70 hydroxyl side chain and the boron atom in the boronate covalent complex of EC19 and BlaC. All three rings of the inhibitor were able to be unambiguously mapped, and Figure 2A shows the model of the bound complex surrounded by the experimental electron density, contoured at 2*σ*.

One of the boronate oxygen atoms interacts with the amide nitrogens of Ser70 and Thr237 (Figure 2B). These two residues constitute the "oxyanion hole" that stabilizes the formation of the anionic, tetrahedral intermediate during *β*-lactam hydrolysis (Scheme 1). The other boronate oxygen occupies the position where the conserved hydrolytic water molecule normally is located. The boronate oxygen atom makes a hydrogen bonding interaction with Glu166, the base normally responsible for activating the water molecule in the deacylation reaction. The

DOI: 10.1021/acsinfecdis.5b00003
ACS Infect. Dis. 2015, 1, 234−242

diketopiperazine substituent (R1) interacts with several active-site residues. The two ketones are positioned by hydrogen bonding along the amide backbone nitrogens of Ser104 and Arg103 while the nearby exocyclic carbonyl interacts with the side chain of Arg171. The central phenol ring points out into the solvent and interacts via hydrogen bonds with a water molecule. The *meta*-benzoic acid R2 substituent similarly points out toward the solvent and does not interact with the enzyme. However, clearly defined electron density is observed in the complex where the carboxylate of other β-lactam complexes normally binds. We have modeled this as a phosphate anion in Figure 2B because the crystallization solution contains 2 M sodium phosphate and this phosphate anion has been observed at this position in the apo-BlaC structure (PDB entry 2GDN).

On the basis of this additional electron density, we advance that in solution the binding of EC19, and other similarly substituted inhibitors, is driven by the interaction of the carboxyl group with R220 and T235, residues that make up the carboxylate binding site. We could obtain a reasonable model of that interaction by simply rotating the methylene group of the *meta*-benzoic acid substituent to optimize the interaction between the carboxyl group and R220 and T235 (Figure 3). This generates two quite reasonable hydrogen bonds at distances of 2.3 and 2.6 Å, respectively. We propose, on the basis of the nature and strength of the inhibition by the inhibitor series studied here, that the initial interaction between EC19 and the enzyme is driven by the binding of the *meta*-benzoic acid group at the carboxyl binding site. This interaction is similar to the formation of a precatalytic Michaelis complex for substrates and positions the boronate atom in close proximity to S70, which, after deprotonation by K73, adds as a nucleophile to the boron atom to generate the covalent enzyme−inhibitor complex. The two boronate oxygen atoms interact with the oxyanion hole residues and the E166 catalytic base in the deacylation reaction. This is followed by the interaction of the diketopiperazine substituent with the amide backbone nitrogens of R103 and S104 and of the carbonyl group with R171. In solution, it is likely that the *meta*-benzoic acid substituent remains bound at the carboxylate binding site and that the alternate inhibitor conformation that we observe in the crystal is likely due to the very high concentration of phosphate in the crystallization buffer solution and the inability of the EC19 benzoic acid substituent to displace it.

Conclusions. We show here that BATSIs can be used as molecular probes to investigate the structural basis of inhibition of BlaC, an important drug target against otherwise drug-resistant strains of tuberculosis. Our major observation is that in addition to an R1 group, the *meta*-benzoic acid substituent in the R2 position is necessary for the effective inhibition of BlaC because it provides productive interactions with the carboxylate binding region of the enzyme. Compound **21** (EC19) was found to have a K_i* of 0.65 μM, which is lower than corresponding values for currently available inhibitors (we have determined the IC_{50} values of clavulanate, sulbactam, and tazobactam to be 1.7 ± 0.2, 1.6 ± 0.2, and 2.5 ± 0.2 μM, respectively[8]). This is the first description of a BATSI inhibitor against BlaC. EC19 may serve as an important lead compound for the rational design of more potent inhibitors. With the insights obtained by this structure−function study, we are confident that further optimization can be reached.

■ METHODS

BlaC Purification. The *blaC* genes carrying a truncated sequence of BlaC cloned in a pET28-based plasmid were expressed in *E. coli* BL21(DE3) and purified; the correct size was confirmed by mass spectrometry as previously described.[6,8] Variant enzymes were generated using site-directed mutagenesis as reported.[8,26] Protein concentrations were determined by measuring the absorption at 280 nm at various dilutions using an Eppendorf BioPhotometer Plus (Eppendorf AG Hamburg, Germany).

BATSI Synthesis. BATSIs were chemically synthesized by the acylation of aminomethaneboronate with suitable commercially available R1-carboxylic acids. Chiral BATSIs were obtained in enantiomerically pure form by the stereoselective homologation of (+)-pinanediol 3-carboxyphenyl-methaneboronate followed by substitution, acylation, and final deprotection at the boronic and carboxylic functionalities. The general scheme for the synthesis of these compounds is summarized in Scheme 2, and experimental details for the synthesis of BATSIs are reported in the Supporting Information (compounds **2**, **5**, **8**, **18**, **20**, **22**, and **23**) or elsewhere (Table 1).

Kinetic Measurements. Steady-state kinetics were studied with an Agilent 8453 diode array spectrophotometer (Palo Alto, CA) in sodium phosphate buffer at room temperature (50 mM, pH 7.2) in a 1 cm path length cuvette as previously detailed. Nitrocefin (NCF) was used as the substrate with an extinction coefficient of $\Delta\varepsilon$ = 17 400 M^{-1} cm^{-1} at 482 nm. Inhibitor kinetics were analyzed with NCF as the reporter substrate at 100 μM concentration. BATSIs follow reversible inhibition kinetics. Increasing concentrations were used to determine the specific concentration K_i that reduces the initial NCF hydrolysis reaction by 50%. For each concentration, reactions were performed in triplicate and the average velocity was used. Results were corrected for NCF affinity using eq 2:

$$K_i(\text{corrected}) = \frac{K_i(\text{obs})}{\left(1 + \frac{[\text{NCF}]}{K_{m\text{NCF}}}\right)} \quad (2)$$

Kinetic parameters for BlaC and reporter substrate NCF were previously determined to be K_m = 56 μM and k_{cat} = 72 s^{-1}.[8] This corresponds to a correction factor of 0.36.

In a first screen, 50 μM inhibitor was used to determine compounds with the ability to reduce the initial velocity of nitrocefin hydrolysis by BlaC by 50%, which would correspond to a "K_i corrected" of 20 μM or less. For all compounds, initial velocities were obtained within 5 s and after 5 min of preincubation. For compounds that possess a stereogenic center on the boron-bearing carbon atom, we gererally observed slow, reversible inactivation resulting in a substantial increase in inhibition after 5 min of preincubation. For compounds which reduced initial velocities by at least half, formal determinations of K_i (immediate) and K_i* (5 min preincubation), respectively, were performed. The results are summarized in Table 1.

In select cases (i.e., compound **21** (EC19)), testing for the reversibility of inhibition was performed as follows: 0.05 μg of BlaC was incubated in 10 μL of buffer with the inhibitor at a concentration equal to 10K_i* for 20 min. Then, the whole reaction mixture was added to 990 μL of buffer solution containing 100 μM NCF, equal to a 1:100 dilution of inhibitor (0.1K_i*). The formation of the NCF product of hydrolysis over

DOI: 10.1021/acsinfecdis.5b00003
ACS Infect. Dis. 2015, 1, 234−242

Table 1. Compounds and Their Corresponding Inhibitor Constants[a]

number	ref	inhibitor	K_i (μM)	K_i* (μM)
		Reference Compounds		
1	11	LP03	>20	>20
2		EC6803	>20	>20
		Penicillin Series		
3	36	EC25 (ampicillin)[b]	>20	13.2 ± 1.7
4	36	GB21 (nafcillin)	>20	>20
5		FP2107 (oxacillin)	>20	>20
		Cephalothin Series		
6	16	LP04	>20	>20
7	16	FP2807[b]	>20	>20
8		CR126[b]	>20	>20
9	24	SM23[b]	>20	1.46 ± 0.2
10	17	EC04	>20	2.76 ± 0.2
		Cefotaxime Compound		
11	11	LP08	5.54 ± 0.3	4.13 ± 0.3
		Ceftazidime Series		
12	15	LP06	>20	>20
13	37	MC35[b]	>20	17.7 ± 2.0
		Cefoperazone Series		
14	12	GB0301	>20	>20
15	12	EC7406	>20	>20
16	12	EC9901	>20	>20
17	12	EC9701	>20	>20
18		EC9001	>20	>20
19	15	CR102	>20	>20
20		COBOR10[b]	>20	3.34 ± 0.4
21	36	EC19[b]	>20	0.65 ± 0.05
		Ureido and Sulfonamido Compounds		
22		CR48	>20	>20
23		FP110216[b]	>20	7.17 ± 0.4
24	17	CR23	>20	>20
25	17	CR100	>20	>20

[a]K_i is the inhibitor concentration that results in a 50% velocity reduction of NCF hydrolysis, corrected for the substrate affinity. K_i* is the corresponding concentration in μM, obtained after preincubation of the enzyme with inhibitor for 5 min (mean of three experiments ± standard error). [b]Indicates compounds that bear two R1 and R2 side groups (compounds with a stereogenic center).

800 s was monitored and compared to a similar experiment without inhibitor.

For EC19, association and dissociation rate constants (k_{on} and k_{off}, respectively) were determined as follows. Product formation was monitored over time in the presence of EC19 in increasing concentrations using 0.05 μg of BlaC and 100 μM NCF. The data were fitted to eq 3 using Origin 8.0 (OriginLab, Northampton, MA) to obtain the apparent rate constant k_{obs}, which reflects the rate of conversion from the initial velocity (v_i) phase to steady-state velocity (v_s), with $A(t)$ indicating the absorbance at reaction time t and A_0 indicating the initial absorbance, respectively:

$$A(t) = A_0 + v_s t + \frac{v_i - v_s}{k_{obs}[1 - \exp(-k_{obs}t)]} \tag{3}$$

For simple (one step) reversible binding to BlaC, k_{obs} is a linear function of inhibitor concentration (eq 4) with

$$k_{obs} = k_{on}[\mathrm{I}] + k_{off} \tag{4}$$

Thus, k_{off} is the $y(0)$ intercept, and k_{on} is derived from slope $k_{obs}/[\mathrm{I}]$, corrected for affinity (eq 5):[27]

$$k_{on} = \frac{k_{obs}}{[\mathrm{I}]\left(1 + \frac{[\mathrm{S}]}{K_m}\right)} \tag{5}$$

An inhibition screen with EC19 (20 μM) was performed for BlaC variant enzymes R220A, R220S, R220A-A244R, and S130G using NCF at 200 μM concentration in order to determine the impact of the carboxylate binding site.[8] The results are summarized in Table 2.

Table 2. BlaC Site-Directed Variant Enzymes[a]

	EC19[21]
R220A	0.96 ± 0.3
R220S	0.96 ± 0.2
R220A, A244R	0.37 ± 0.2
S130G	<0.1

[a]Fractional velocities (v/v_0) of NCF hydrolysis following 5 min of preincubation with inhibitor EC19 at 20 μM concentration, in relation to uninhibited reaction, performed in triplicate. Note that the catalytic efficiency of the variant enzymes is significantly impaired compared to the wild type, with the k_{cat}/K_m ratio (in μM^{-1} s^{-1}) for NCF of 0.01 (R220A, R220S), 0.02 (S140G), 0.1 (R220A, A244R), and 1.34 (wild type), respectively.[8] The S130G variant enzyme was completely inhibited by EC19.

Crystallography. The method of hanging drop vapor diffusion was used for the crystallization of N172A mutant BlaC. The composition of the well consists of 0.1 M HEPES, pH 7.5 and 2 M $NH_4H_2PO_4$, which makes the final pH of the well solution 4.1. Protein at a concentration of 14 mg/mL was mixed 1:1 with the well solution and incubated at 10 °C. N172A BlaC was initially seeded with the native enzyme crystals (BlaC), and then after iterative crystal seeding, the pure mutant crystals were obtained. Iterative microseeding resulted in efficient crystal growth as well as improved morphology and finally produced diffraction-quality crystals of the mutant enzyme. N172A crystals were solved in same space group ($P2_12_12_1$) as the wild type and were larger.

Data Collection and Refinement. EC19 is insoluble in water but soluble in DMSO. A DMSO solution of 500 mM EC19 was used as a stock solution and serially diluted with an equal volume of water for three rounds of soaking. This diluted DMSO solution (containing about 65 mM EC19) was used for the soaking experiment with N172A variant BlaC. After placement in the soaking solution, the crystals were frozen in liquid nitrogen in time intervals of 15 and 30 min and 1, 2, 4, 6, 12, 24, and 48 h. Mineral oil was added to the solution as a cryoprotectant. Diffraction data were collected from each of the single frozen crystals using a RAXIS-IV++ detector mount on a Rigaku RH-200 rotating anode (copper anode) X-ray generator. Whereas no or insufficient electron density of the ligand was observed for crystals after early freezing, adequate intensity was observed for crystals frozen after 24 h of soaking. Data were collected at Brookhaven National Laboratory on crystals frozen after 24 h of soaking with EC19. Beamline X29 was used for data collection. The data were processed using HKL2000.[28] The previous structure of Mtb β-lactamase with bound NXL104 (or avibactam) (PDB entry 4HFX)[29] was used to phase the data using the CCP4 software suite.[30] Multiple rounds of structural refinement and model building were

DOI: 10.1021/acsinfecdis.5b00003
ACS Infect. Dis. 2015, 1, 234−242

performed in Refmac5,[31,32] Phenix,[33] and Coot.[34] Structure figures were generated using PyMOL (The PyMOL Molecular Graphics System, version 1.3, Schrödinger, LLC) and ChemDraw Ultra 12.0.[35] Atomic coordinates and experimental structure factors have been deposited in the Protein Data Bank (PDB entry 4X6T). Table 3 lists the data collection statistics for the structures as well as the final refinement statistics.

Table 3. Summary of Data Collection and Refinement Statistics for the N186Ala -BlaC-EC19 Complex

data collection statistics	
X-ray source	NSLS beamline X-29
date of collection	2013-09-20
wavelength (Å)	1.0 (single wavelength)
temperature (K)	100
resolution range	38.5−1.40
reflection	50 722
completeness	91.67 (100)
redundancy	6.5
I/sigma (σ)	3.05
space group	$P2_12_12_1$
Unit Cell (Å)	
A	43.26
B	71.42
C	84.68
$\alpha = \beta = \Upsilon$	90.00°
molecules per a.u.	1
Refinement	
refinement program	PHENIX
R_{work} (%)	16.60
R_{free} (%)	20.20
$R_{free\ test\ set}$	1993 reflections (4.13%)
estimated twining fraction	no twining to report
Atoms	
total number of atoms	2341
average *B* factor	20.0
protein (chain A)	2005
phosphate (chain P)	35
EC19 (chain E)	38
water (chain W)	263
rms Deviation	
bond length (Å)	0.006
bond angle (deg)	1.283
pdb accession code	4X6T

■ ASSOCIATED CONTENT

Supporting Information

The following file is available free of charge on the ACS Publications website at DOI: 10.1021/acsinfecdis.5b00003.

Figures S1A,B and S2A,B and descriptions of the synthesis of compounds.

Accession Codes

The Protein Data Bank entry for the BlaC-EC19 adduct is 4X6T.

■ AUTHOR INFORMATION

Corresponding Authors

*E-mail: fabio.prati@unimore.it.
*E-mail: john.blanchard@einstein.yu.edu.
*E-mail: robert.bonomo@va.gov.

Author Contributions

S.G.K. and S.H. contributed equally to this article.

Notes

The authors declare no competing financial interest.

■ ACKNOWLEDGMENTS

Research reported in this publication was supported by the National Institute of Allergy and Infectious Diseases of the National Institutes of Health under award numbers R01AI100560 and R01AI063517 (to R.A.B.) and NIH AI060899 (to J.S.B.). The content is solely the responsibility of the authors and does not necessarily represent the official views of the National Institutes of Health. This study was supported in part by funds and/or facilities provided by the Cleveland Department of Veterans Affairs, Veterans Affairs Merit Review Program Award 1I01BX001974, and the Geriatric Research Education and Clinical Center VISN 10 (to R.A.B.). Parts of this study were presented in the form of an abstract (European Congress of Clinical Microbiology and Infectious Diseases, Milan 2011, American Thoracic Society, San Diego 2014).

■ REFERENCES

(1) Hong-Kong-Chest-Service/British-Medical-Research-Council (1991) Controlled trial of 2, 4, and 6 months of pyrazinamide in 6-month, three-times-weekly regimens for smear-positive pulmonary tuberculosis, including an assessment of a combined preparation of isoniazid, rifampin, and pyrazinamide. Results at 30 months. Hong Kong Chest Service/British Medical Research Council. *Am. Rev. Respir. Dis. 143*, 700−706.

(2) Singapore-Tuberculosis-Service/British-Medical-Research-Council (1991) Assessment of a daily combined preparation of isoniazid, rifampin, and pyrazinamide in a controlled trial of three 6-month regimens for smear-positive pulmonary tuberculosis. Singapore Tuberculosis Service/British Medical Research Council. *Am. Rev. Respir. Dis. 143*, 707−712.

(3) Combs, D. L., O'Brien, R. J., and Geiter, L. J. (1990) USPHS Tuberculosis Short-Course Chemotherapy Trial 21: effectiveness, toxicity, and acceptability. The report of final results. *Ann. Int. Med. 112*, 397−406.

(4) WHO; Multidrug and Extensively Drug-Resistant TB (M/XDR-TB): 2010 Global Report on Surveillance and Response.

(5) Chambers, H. F., Moreau, D., Yajko, D., Miick, C., Wagner, C., Hackbarth, C., Kocagoz, S., Rosenberg, E., Hadley, W. K., and Nikaido, H. (1995) Can penicillins and other beta-lactam antibiotics be used to treat tuberculosis? *Antimicrob. Agents Chemother. 39*, 2620−2624.

(6) Wang, F., Cassidy, C., and Sacchettini, J. C. (2006) Crystal structure and activity studies of the Mycobacterium tuberculosis beta-lactamase reveal its critical role in resistance to beta-lactam antibiotics. *Antimicrob. Agents Chemother. 50*, 2762−2771.

(7) Hugonnet, J. E., Tremblay, L. W., Boshoff, H. I., Barry, C. E., 3rd, and Blanchard, J. S. (2009) Meropenem-clavulanate is effective against extensively drug-resistant Mycobacterium tuberculosis. *Science 323*, 1215−1218.

(8) Kurz, S. G., Wolff, K. A., Hazra, S., Bethel, C. R., Hujer, A. M., Smith, K. M., Xu, Y., Tremblay, L. W., Blanchard, J. S., Nguyen, L., and Bonomo, R. A. (2013) Can Inhibitor-Resistant Substitutions in the Mycobacterium tuberculosis beta-Lactamase BlaC Lead to Clavulanate Resistance?: a Biochemical Rationale for the Use of beta-Lactam-beta-Lactamase Inhibitor Combinations. *Antimicrob. Agents Chemother. 57*, 6085−6096.

(9) Kurz, S. G., Bonomo, R. A. Reappraising the use of beta-lactams to treat tuberculosis. *Expert Rev. Anti-Infect. Ther. 10*, 999−1006.10.1586/eri.12.96

(10) Ness, S., Martin, R., Kindler, A. M., Paetzel, M., Gold, M., Jensen, S. E., Jones, J. B., and Strynadka, N. C. (2000) Structure-based

DOI: 10.1021/acsinfecdis.5b00003
ACS Infect. Dis. 2015, 1, 234−242

design guides the improved efficacy of deacylation transition state analogue inhibitors of TEM-1 beta-Lactamase(,). *Biochemistry 39*, 5312−5321.

(11) Thomson, J. M., Prati, F., Bethel, C. R., and Bonomo, R. A. (2007) Use of novel boronic acid transition state inhibitors to probe substrate affinity in SHV-type extended-spectrum beta-lactamases. *Antimicrob. Agents Chemother. 51*, 1577−1579.

(12) Ke, W., Sampson, J. M., Ori, C., Prati, F., Drawz, S. M., Bethel, C. R., Bonomo, R. A., and van den Akker, F. (2011) Novel insights into the mode of inhibition of class A SHV-1 beta-lactamases revealed by boronic acid transition state inhibitors. *Antimicrob. Agents Chemother. 55*, 174−183.

(13) Chen, Y., Shoichet, B., and Bonnet, R. (2005) Structure, function, and inhibition along the reaction coordinate of CTX-M beta-lactamases. *J. Am. Chem. Soc. 127*, 5423−5434.

(14) Morandi, F., Caselli, E., Morandi, S., Focia, P. J., Blazquez, J., Shoichet, B. K., and Prati, F. (2003) Nanomolar inhibitors of AmpC beta-lactamase. *J. Am. Chem. Soc. 125*, 685−695.

(15) Drawz, S. M., Babic, M., Bethel, C. R., Taracila, M., Distler, A. M., Ori, C., Caselli, E., Prati, F., and Bonomo, R. A. (2010) Inhibition of the class C beta-lactamase from Acinetobacter spp.: insights into effective inhibitor design. *Biochemistry 49*, 329−340.

(16) Morandi, S., Morandi, F., Caselli, E., Shoichet, B. K., and Prati, F. (2008) Structure-based optimization of cephalothin-analogue boronic acids as beta-lactamase inhibitors. *Bioorg. Med. Chem. 16*, 1195−1205.

(17) Eidam, O., Romagnoli, C., Caselli, E., Babaoglu, K., Pohlhaus, D. T., Karpiak, J., Bonnet, R., Shoichet, B. K., and Prati, F. (2010) Design, synthesis, crystal structures, and antimicrobial activity of sulfonamide boronic acids as beta-lactamase inhibitors. *J. Med. Chem. 53*, 7852−7863.

(18) Doucet, N., De Wals, P. Y., and Pelletier, J. N. (2004) Site-saturation mutagenesis of Tyr-105 reveals its importance in substrate stabilization and discrimination in TEM-1 beta-lactamase. *J. Biol. Chem. 279*, 46295−46303.

(19) Bethel, C. R., Hujer, A. M., Hujer, K. M., Thomson, J. M., Ruszczycky, M. W., Anderson, V. E., Pusztai-Carey, M., Taracila, M., Helfand, M. S., and Bonomo, R. A. (2006) Role of Asp104 in the SHV beta-lactamase. *Antimicrob. Agents Chemother. 50*, 4124−4131.

(20) Ke, W., Bethel, C. R., Thomson, J. M., Bonomo, R. A., and van den Akker, F. (2007) Crystal structure of KPC-2: insights into carbapenemase activity in class A beta-lactamases. *Biochemistry 46*, 5732−5740.

(21) Drawz, S. M., and Bonomo, R. A. (2010) Three decades of beta-lactamase inhibitors. *Clin. Microbiol. Rev. 23*, 160−201.

(22) Marciano, D. C., Brown, N. G., and Palzkill, T. (2009) Analysis of the plasticity of location of the Arg244 positive charge within the active site of the TEM-1 beta-lactamase. *Protein Sci. 18*, 2080−2089.

(23) Wang, X., Minasov, G., Blazquez, J., Caselli, E., Prati, F., and Shoichet, B. K. (2003) Recognition and resistance in TEM beta-lactamase. *Biochemistry 42*, 8434−8444.

(24) Thomson, J. M., Distler, A. M., Prati, F., and Bonomo, R. A. (2006) Probing active site chemistry in SHV beta-lactamase variants at Ambler position 244. Understanding unique properties of inhibitor resistance. *J. Biol. Chem. 281*, 26734−26744.

(25) Hugonnet, J. E., and Blanchard, J. S. (2007) Irreversible inhibition of the Mycobacterium tuberculosis beta-lactamase by clavulanate. *Biochemistry 46*, 11998−12004.

(26) Hujer, A. M., Hujer, K. M., Helfand, M. S., Anderson, V. E., and Bonomo, R. A. (2002) Amino acid substitutions at Ambler position Gly238 in the SHV-1 beta-lactamase: exploring sequence requirements for resistance to penicillins and cephalosporins. *Antimicrob. Agents Chemother. 46*, 3971−3977.

(27) Copeland, R. A. *Evaluation of Enzyme Inhibitors in Drug Discovery*; John Wiley & Sons, 2005.

(28) Otwinowski, Z., and Minor, W. (1997) Processing of X-ray Diffraction Data Collected in Oscillation Mode. *Methods Enzymol. 276*, 307−326.

(29) Xu, H., Hazra, S., and Blanchard, J. S. (2012) NXL104 irreversibly inhibits the beta-lactamase from Mycobacterium tuberculosis. *Biochemistry 51*, 4551−4557.

(30) Potterton, E., Briggs, P., Turkenburg, M., and Dodson, E. (2003) A graphical user interface to the CCP4 program suite. *Acta Crystallogr., D 59*, 1131−1137.

(31) Murshudov, G. N., Vagin, A. A., and Dodson, E. J. (1997) Refinement of macromolecular structures by the maximum-likelihood method. *Acta Crystallogr., D 53*, 240−255.

(32) Pannu, N. S., Murshudov, G. N., Dodson, E. J., and Read, R. J. (1998) Incorporation of prior phase information strengthens maximum-likelihood structure refinement. *Acta Crystallogr., D 54*, 1285−1294.

(33) Adams, P. D., Afonine, P. V., Bunkoczi, G., Chen, V. B., Davis, I. W., Echols, N., Headd, J. J., Hung, L. W., Kapral, G. J., Grosse-Kunstleve, R. W., McCoy, A. J., Moriarty, N. W., Oeffner, R., Read, R. J., Richardson, D. C., Richardson, J. S., Terwilliger, T. C., and Zwart, P. H. (2010) PHENIX: a comprehensive Python-based system for macromolecular structure solution. *Acta Crystallogr., D 66*, 213−221.

(34) Emsley, P., and Cowtan, K. (2004) Coot: model-building tools for molecular graphics. *Acta Crystallogr., D 60*, 2126−2132.

(35) Mills, N. (2006) ChemDraw Ultra 10.0. *J. Am. Chem. Soc. 128*, 13649−13650.

(36) Winkler, M. L., Rodkey, E. A., Taracila, M. A., Drawz, S. M., Bethel, C. R., Papp-Wallace, K. M., Smith, K. M., Xu, Y., Dwulit-Smith, J. R., Romagnoli, C., Caselli, E., Prati, F., van den Akker, F., and Bonomo, R. A. (2013) Design and exploration of novel boronic acid inhibitors reveals important interactions with a clavulanic acid-resistant sulfhydryl-variable (SHV) beta-lactamase. *J. Med. Chem. 56*, 1084−1097.

(37) Kotsakis, S. D., Caselli, E., Tzouvelekis, L. S., Petinaki, E., Prati, F., and Miriagou, V. (2013) Interactions of oximino-substituted boronic acids and beta-lactams with the CMY-2-derived extended-spectrum cephalosporinases CMY-30 and CMY-42. *Antimicrob. Agents Chemother. 57*, 968−976.

DOI: 10.1021/acsinfecdis.5b00003
ACS Infect. Dis. 2015, 1, 234−242